VOL. 17, NO. 16, AUGUST 2022 ISSN 1819-6608
ARPN Journal of Engineering and Applied Sciences

www.arpnjournals.com

NUMERICAL SIMULATION OF EFFECT OF ARTIFICIAL REEF ARRANGEMENTS ON WAKE REGION CHARACTERISTIC AROUND THE COMBINED TUBE REEF WITH ZIG-ZAG FORMATION

Mohammad Tauviqirrahman[1], Sugiyanto[1], Khoirul Ma'nun[1], Jamari[1], Muchammad[1] and Paryanto[1,2]
[1]Department of Mechanical Engineering, Faculty of Engineering, Diponegoro University, Semarang, Central Java, Indonesia
[2]Institute for Factory Automation and Production Systems (FAPS), Friedrich-Alexander-Univerftablesität Erlangen-Nürnberg, Egerlandstr, Erlangen, Germany
E-Mail: mtauviq99@lecturer.undip.ac.id

ABSTRACT

Around the world, there has been an increasing tendency toward the use of artificial reefs (ARs) to enhance recreational opportunities and offer coastal protection. The placement of artificial reefs (ARs) on the seafloor in a variety of configurations results in a range of flow characteristics. The first parameters that contribute to the best hydrodynamic qualities in terms of the ARs layout remain unknown. The present work conducts numerical research on the hydrodynamics of ARs with three rows, with a particular emphasis on how to enhance the complicated wake region when the spacing between the reefs varies. The tube artificial reef system with zig-zag formation is investigated using a complete three-dimensional computational fluid dynamics (3D CFD) technique using the renormalization group (RNG) k-εturbulent model. Through several numerical simulations, it is found that the configuration of the reef groups with spacing between tubes of 1.5 D has the greatest effect on the wake region. Additionally, to minimize beach erosion, the ARs should be deployed 10 meters from the shoreline. This study establishes a scientific basis for the arrangement of artificial reefs and their relationship to the shoreline.

Keywords: artificial reef (AR), computational fluid dynamics (CFD), flow 3D, wake region.

1. INTRODUCTION

When placed in the sea, artificial reefs (ARs) have been extensively employed to boost overall biomass production, including fish [1]. Recent studies have demonstrated the considerable effect of flow fields surrounding reefs both ecologically and hydrodynamically. Ontowirjo and Armono [2] observed the hydrodynamic parameters (i.e. particle velocities, fluid flows, wave breaking, and dissipation of wave energy) of a specially shaped submerged structure in order to reduce the energy of offshore waves and to provide a safe and productive environment for fish, using a numerical modeling approach. By simulating regular and irregular waves, Zhen-qing and Yong-he [3] investigated the effects of water depth on the hydrodynamic force of the artificial reef. They discovered that in ultra-shallow water, the hydrodynamic force increases significantly as water depth decreases. Zhaoyang *et al.* [4-5] investigated the hydrodynamic properties of an artificial reef using a numerical method, namely CFD (computational-fluid-dynamics) and discovered that the numerical simulation findings are in good agreement with the experimental data. As a result, they proposed that the CFD method may be used to forecast the hydrodynamic behavior of artificial reefs. Another intriguing conclusion was reached by Woo *et al*. [6]. The authors used numerical analysis to analyze 24 types of artificial reefs constructed in South Korea in terms of drag coefficient and wake regions. Later, Kim et al. [7] conducted additional studies concentrating not only on drag coefficients but also on the wake region and structural response of general artificial reefs in order to increase the attraction of marine bio-organisms and water flow stability. One emerging conclusion from these investigations is that using numerical modeling to create the appropriate flow characteristics around artificial reefs is a practical technique.

The shape of the artificial reef, which has a substantial effect on the flow fields, has also garnered much interest from engineers and marine ecologists. Liu *et al.* [8] investigated the flow fields within and around a hollow cube artificial reef by altering the size of the hollows. Later, Liu *et al.* [9] further investigated the flow field features surrounding star-shaped artificial reefs. They discussed the effect of arrangement and spacing on the flow field of one and two artificial reefs in their article. Yaakob *et al.* [10] presented a novel design for artificial reefs (ARs) based on the concept of a cycling helmet. To investigate the effect of such designs on the flow pattern, they used hollow cube ARs in their studies. In terms of upwelling generation, Jiang *et al*. [11] used the CFD method to analyze the flow field created by the guide plate installation on artificial reefs. The authors confirmed that placing the guide plate considerably improves the production of upwelling and the width of the wake region.According to Jiao *et al*. [12], the tube shape of artificial reefs can have a considerable ecological effect on fish aggregation through numerical simulation and PIV experiments. Additionally, it was discovered that when five reefs are included and the ratio of reef unit height to water depth is 0.224, a higher unit artificial reef effect is obtained. Wang *et al*. [13] recently published a study on the effects of cut-opening ratio, cut-opening form, and cut-opening number on upwelling and back eddies in the design of a cubic artificial reef. The ideal design of cubic

artificial reefs was discovered as a consequence of their work and could be used as a scientific reference. Furthermore, several researchers demonstrated that the arrangement of the artificial reefs could change the flow field surrounding the artificial reefs. The key problem for ecological engineers is the successful deployment of ARs to develop higher marine ranching. Lan and Hsui [14] developed a complete mathematical model as well as a concrete technique for establishing artificial reefs within a limited budget. Suzuki *et al*. [15] developed new and effective coral restoration procedures for larval seeding while also understanding the nuances of reef-building corals' early life stages. Based on a CFD flow simulation approach, Liu and Su [16] offered an in-depth analysis of various flow patterns of different reef block layouts to consolidate the artificial reef deployment strategy. They discovered that artificial reefs should be properly separated and built in a longitudinal layout parallel to the current direction. Zheng *et al*. [17] used numerical simulation and experimentation to investigate the effect of disposal space on the flow field around two reefs. The best disposal space has been highlighted in both the vertical and parallel combinations of the artificial reef arrangement.

When performing a literature survey, one also can find that most of the previously published works used the artificial reef (AR) as a single module/block, not as a system containing multiple rows of ARs as adopted in the present work. It is hypothesized here that the multiple rows of AR lead to the what-so-called collective effects of the block of AR which are more effective compared to the single module of AR based on the work of Liu and Su [16]. Therefore, following the mainframe of the optimal arrangement of the artificial reefs (ARs), the main aim of this study is to investigate the effect of arrangement on the flow field of an artificial reef in terms of the wake region. In this way, the deployment of the ARs can be more appropriately conducted concerning the shoreline for achieving better coast abrasion countermeasure. In this research, the tube shape of ARs is chosen according to the work of Jiao *et al*. [12]. For computation, the ARs are characterized by three rows of tube ARs with zig-zag formation. How spacing of such formation affects the flow field is of particular interest as well as the length of the AR block both in the lateral or transversal direction. The numerical model is based on a solution of the equations governing momentum and conservation of mass for an incompressible, Newtonian fluid. In this way, with the development of the computational fluid dynamic (CFD) approach, much information measured barely by the experimental method can be clearly performed by the computer simulation. This research can provide a scientific reference for the optimal formation of the artificial reefs with respect to the reduction in beach erosion.

2. METHODOLOGY

2.1 Governing Equation

A Newtonian fluid with a constant density is expected to be present in the water flow in the simulation, which is supposed to be incompressible and viscous. The flow is in an unsteady state, and there are no heat exchanges taking place. On the basis of the continuity equation, water flow velocity calculations are performed. The momentum equation is derived from the three-dimensional Reynolds-average Navier-Stokes (RANS) equation. Accordingly, below is a list of the equations [18].

The continuity equation:

$$\frac{\partial \rho}{\partial t} + \frac{\partial}{\partial x_i}(\rho u_i) = 0 \quad (1)$$

The momentum equation:

$$\frac{\partial}{\partial t}(\rho u_i) + \frac{\partial}{\partial x_i}(\rho u_i u_j) = -\frac{\partial p}{\partial x_i} + \frac{\partial}{\partial x_j}\left[\mu \frac{\partial u_i}{\partial} - \rho \overline{u_i' u_j'}\right] + S_i \quad (2)$$

In Eqs. (1–2), ρ is the density of the fluid; u_i and u_j are the average velocity components for x, y, z; p is the static hydrodynamic pressure; μ is the viscosity; u_i' and u'_j are the fluctuation velocities; $-\rho\ \overline{u_i' u'_j}$ is the Reynolds stress; i, j=1, 2, 3 (x, y, z) and S_i is the source item.

The renormalization group (RNG) k-εturbulence model is used in this paper. This is an enhancement to the k-ε turbulence model. The following are the new turbulence equations for k and ε [18]:
k equation:

$$\frac{\partial(\rho k)}{\partial t} + \frac{\partial(\rho k u_i)}{\partial x_i} = \frac{\partial}{\partial x_j}\left[\alpha_k \mu_{eff} \frac{\partial k}{\partial x_j}\right] + G_k + \rho\varepsilon \quad (3)$$

ε equation:

$$\frac{\partial(\rho \varepsilon)}{\partial t} + \frac{\partial(\rho \varepsilon u_i)}{\partial x_i} = \frac{\partial}{\partial x_j}\left[\alpha_k \mu_{eff} \frac{\partial \varepsilon}{\partial x_j}\right] + C_{1\varepsilon}^* \frac{\varepsilon}{k} G_k - C_{2\varepsilon}^* \rho \frac{\varepsilon^2}{k} \quad (4)$$

Where $G_k$is defined by the average flow gradient based on the turbulent kinetic energy, μ_{eff} is the validity turbulent viscosity coefficient, α_k and α_ε are the inverse turbulent Prandtl numbers for the *k*and *ε* equations, and $C_{1\varepsilon}$ and $C_{2\varepsilon}$ are known constants.

2.2 CFD Model

In the present study, the multi-array artificial reef configuration consisting of three rows of artificial reefs is developed. The structures of three rows tube artificial reef models are reflected in Figure-1. In the present study, for the computation, the zig-zag formation of tube artificial reefs is applied, as shown in Figure-2. The shape of the artificial reef chosen is the tube with a diameter *D of* 1 meter. The velocity in the simulation corresponds to the

actual velocity, which is 1 m/s. As is known, the real sea current velocity is less than 1 m/s according to velocity measurement by Acoustic Doppler Current Profilers (ADCP) in seawater. In detail, Table-1 shows the geometry of the computational domain concerning the shoreline and the inclination slope of the shore. For all following computations, the dimension is set to D unit. The inclination slope of shore, θ is set to constant, i.e. 2.73°.

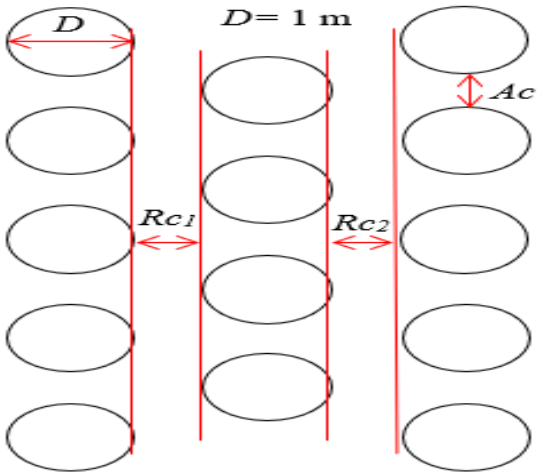

Figure-1. Artificial reef pattern with zig-zag formation.

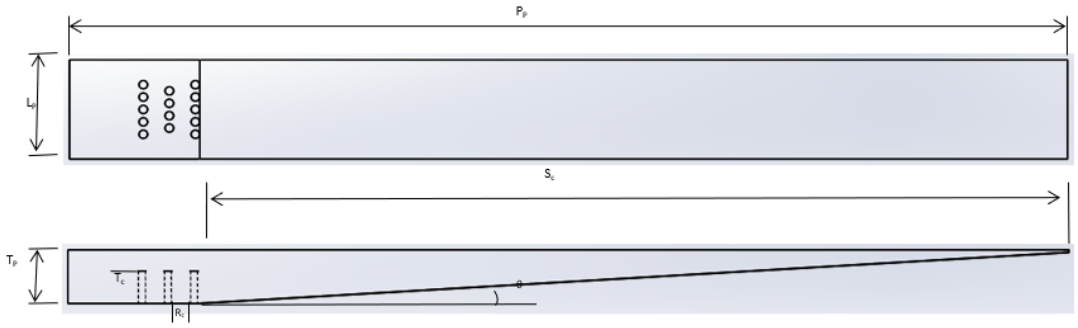

Figure-2. Schematic representation of the computational domain, which contains three rows of artificial reefs with zig-zag formation in both horizontal and vertical perspectives.

Table-1. The parameters employed in this simulation.

Variable	Unit (in*D*)
Length of shoreline, P_p	115
Width of shoreline, L_p	-
Shore depth, T_p	5
Height of artificial reef, *Tc*	3
Distance of artificial reef to shore, S_c	100
Distance between the edges of the artificial reef line, R_c	0.5, 1, 2, 3
Distance between the edges of the artificial reef line, A_c	0.5
Diameter of an artificial reef, *Ø*	*1*

The computational grid is created based on ANSYS. The finite volume method is used to discretize the three-dimensional unsteady incompressible Navier-Stokes equation. For the pressure-based solver, a first-order implicit formulation is employed. To solve the pressure and velocity coupling, the SIMPLEC algorithm is utilized. A second-order upwind discretization approach is utilized for the convection terms in the momentum, turbulent kinetic energy, and turbulent energy dissipation rate equations.

3. RESULTS AND DISCUSSIONS

To aim the research purposes, CFD simulations are used to examine the flow fields represented by velocity profiles for a variety of artificial reef arrangements. Analysis of the effects of zig-zag spacing in the artificial reef pattern on wake region is carried out in great depth here. Tube-based artificial reefs with different spacing between AR units are covered in this section. In this study, the distance between the edges of the artificial reef (A_c), the distance between the edges of the first row 1 (R_{c1}), and the distance between the edges of the second row (R_{c2}) are varied.

Figure-3 compares slow wake regions for various arrangements with different R_c values in the case of the artificial reef with three rows. In this study, it is assumed that the same spacing is used on the second and third rows of the artificial reef units. It means that the R_{c1} value is equal to the R_{c2} value. Based on Figure-3, the simulation results indicate that increasing R_c has little effect on the contour of the velocity profile as well as the length of the slowwake region. The slow wakeregion generated refers to a single larger zone that connects each artificial reef unit.

From an ecological and hydrodynamic standpoint, this creates the best conditions for fish and the bio-ecosystem. In terms of the length of the slow wake region, the artificial reef formations with different R_c values predict the same value, i.e. 6 m. This is the desired condition for preventing beach abrasion. Because of the large length of the slow wake region, it is possible to deploy the artificial reef in real-time. If the artificial reef is placed properly, the back velocity from the beach will be minimized, preventing the sand from being carried to the middle of the sea by the waves.In general, as shown in Figure-3, the smaller the value of R_c, the greater the distance at which the velocity declines. When the distance between the edges of the current-resisting column (R_c) equals 0.5D, the area of the greatest speed reduction occurs. According to Figure-3, the arrangement and spacing of artificial reef units have a significant effect on the velocity distribution (i.e. slow wake zone) within and around the artificial reef.

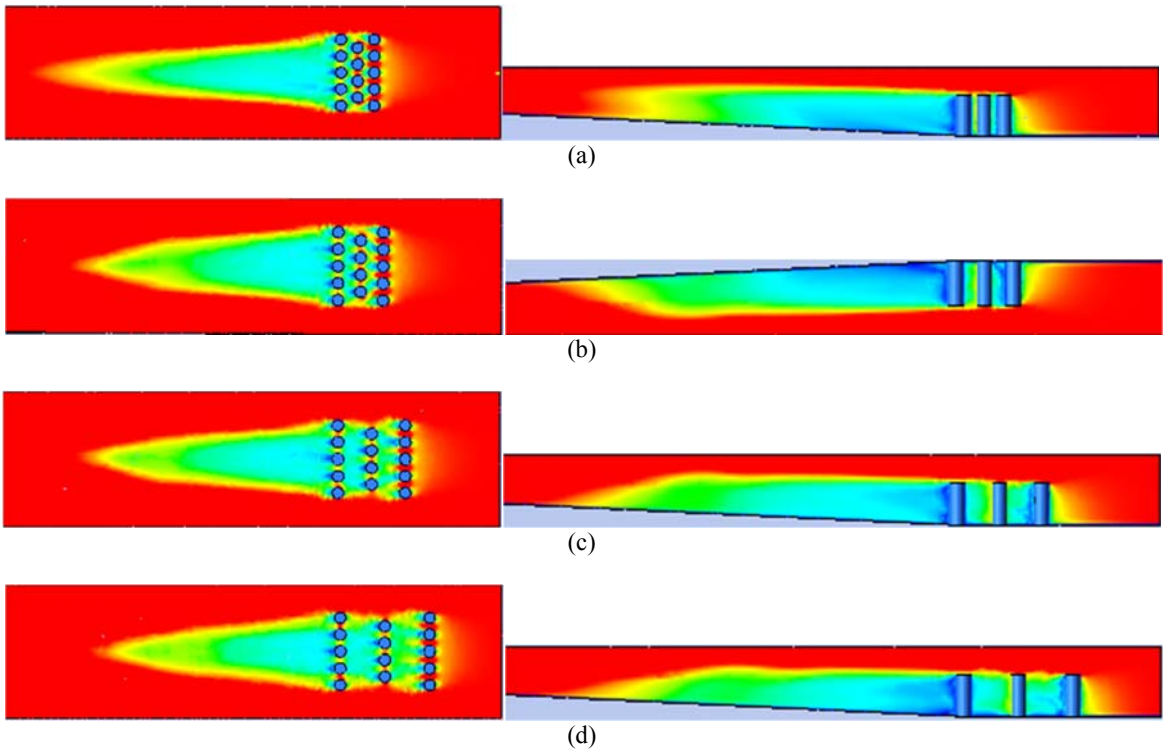

Figure-3. Contour of velocity profile varying thedistance between the edges of the AR rows R_c. (a), R_{c1}=R_{c2}=0.5, (b) R_{c1}=R_{c2}=1, (c) R_{c1}=R_{c2}=2, and (d) R_{c1}=R_{c2}=3. Note: All results are evaluated at A_c=0.5.*Left*: top view, *Right*: front view.

Table-2 details the length of the slow wake region and the minimum velocity within the slow wake region for each artificial reef formation. For these calculations, to determine the velocity and distance of the lowest velocity drop, a straight line is drawn from the inlet's end to a 50-meter distance, as shown in Figure-4. It should be noted that in the computations, five simulations are carried out, where each simulation only varies the distance between the lines (R_{c1}) and the distance between the lines (R_{c1}). From the previous simulation results, it is found that the most effective A_C distance was at a distance of 0.5D. Maintaining flow with a distance of A_c, R_{c1}, and R_{c2}: the closer the three components are, the slower the velocity and the greater the distance. It is also observed that the most effective results are obtained at a distance of A_c = 0.5D, R_{c1} = 0.5D, and R_{c2} = 0.5D, with a minimum speed of 0.235 m/s at a distance of 10 meters behind the artificial reef. From Table 2, it can be seen that the lowest minimum velocity of0.235 m/s occurs at a distance of 0.5 x 0.5 x 0.5 D. It seems that the artificial reef is quite effective in reducing the velocity by up to 76.5% from the initial velocity of 1 m/s at the furthest distance of 10 meters as shown in Figure-5. So it can be concluded that the smaller the distance between the current retainers, the more effective the decrease in velocity will be and the minimum speed distance will be further away.

In detail, Figure-5 depicts the decrease in velocity at a distance of 0.5 x 0.5 x 0.5 D, with the velocity analysis line in the center of the formation, 37 meters from the last line of the artificial reef and 2 meters above the seabed. When the input flow velocity of 1 m/s collides with the mounted current reef, the speed decreases. When the flow encounters artificial reefs at rows 1 and 3, its velocity reduces and then climbs from 0 m/s to 0.238 m/s for a distance of up to 1 meter behind breakwater 3. Following an increase in velocity, the flow velocity decreases again in the deceleration zone until it reaches an ideal point 10 meters after the artificial reef row of 3. At a

distance of ten meters behind the artificial reef row of 3, the best velocity reduction is 0.235 m/s or 76.5 percent of the beginning speed of one m/s.

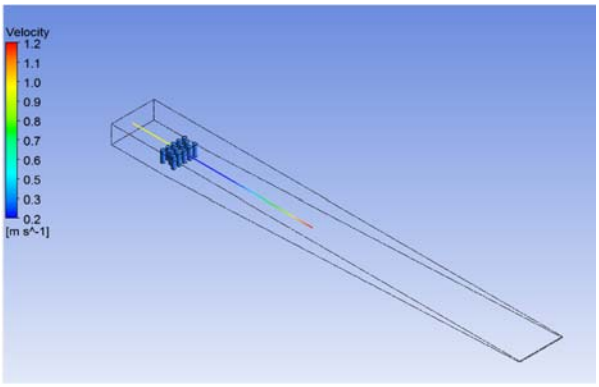

Figure-4. Base-line of velocity analysis.

Table-2. Characteristics of flow for various configurations and spacings of artificial reefs.

AR formation (*D*)			Velocity (m/s)	Length of wake region (m)
A_c	R_{c1}	R_{c2}		
0.5	0.5	0.5	0.235	10
0.5	1	1	0.237	10
0.5	2	2	0.239	10
0.5	3	3	0.242	10
0.5	4	4	0.249	10

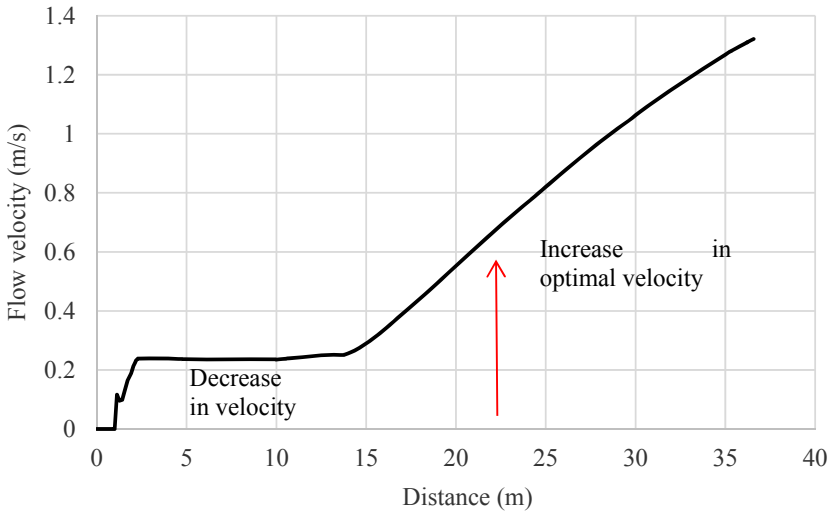

Figure-5. Flow velocity at distance of 0.5 x 0.5 x 0.5*D*.

From a physical standpoint, the flow current that is obstructed by the artificial reef will change direction and velocity. To investigate this phenomenon, changes in direction and velocity can be represented as velocity vector lines, as seen in Figure-6 below. Figure-6 shows that when the flow travels through the reef, there is an area of flow buildup and vortex formation. Flow accumulation happens when water passes through a narrower gap, resulting in a flow queue. The vortex forms as a result of the backflow behind the barrier, resulting in a turbulent flow. In this scenario, the length of the turbulent area is 1*D* away.

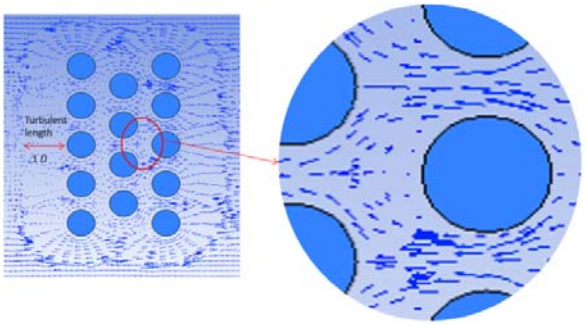

Figure-6. Velocity vector of artificial reefs with three rows pattern in the horizontal view.

Figure-7 depicts the direction of velocity vector's when viewed from the front plane. Because of the presence of obstructions, the fluid can be seen to change direction. As seen in Figure-7, there is backflow at the

back of the barrier. The fluid that initially flows perpendicular to the barrier is reflected towards the top of the barrier, resulting in a lower velocity in the area behind the barrier than in the fluid flow over the barrier.

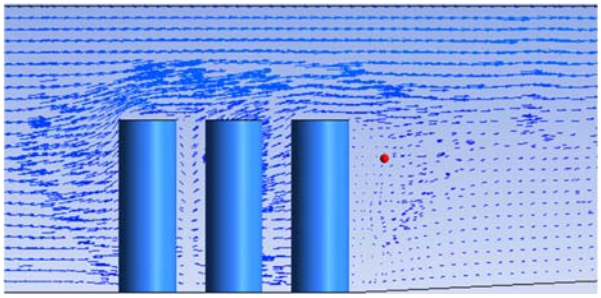

Figure-7. Velocity vector of artificial reefs with three rows in the vertical view.

4. CONCLUSIONS

In the present paper, the feasibility of the artificial reef was estimated through the length of the wake region. The effect of the zig-zag formation of the artificial reef on the flow characteristic surrounding reef was investigated. The pattern with three rows of tube artificial reef was studied varying the length of the rows both in longitudinal and transversal direction. The CFD (Computational Fluid Dynamics) method is used to characterize the velocity profiles surrounding reef. The following conclusions can be drawn as follows:

a) The tighter the artificial reefsis, the better the velocity drop and the shorter the space between the velocity drops.
b) The lowest velocity is attained using a configuration with A_c=0.5 D, R_{c1} =0.5 D, and R_{c2}= 0.5 D.
c) At a distance of 10 meters behind the final row of artificial reef, the magnitude of the lowest velocity in the best formation (i.e.A_c=0.5 D, R_{c1} =0.5 D, and R_{c2}= 0.5 D) is 0.235 m/s (76.5 percent of the original current velocity).

ACKNOWLEDGMENT

This research is fully supported by RPI (Research Publication International) grant, No.831.1 - 01/UN7.P4.3/PP/2019. The authors fully acknowledged Institute for Research and Community Services (LPPM), Universitas Diponegoro for the approved fund which makes this important research viable and effective.

REFERENCES

[1] Bohnsack J.A. and Sutherland D.L. 1985. Artificial Reef Research: A Review with Recommendations for Future Priorities. Bulletin of Marine Science. 37(1): 11-39.

[2] Ontowirjo B., and Armono H.D. 2003. Artificial Reef Methodology for Coastal Protection Using Submerged Structures: A Numerical Modeling Approach. In: Goudas C., Katsiaris G., May V., Karambas T. (eds) Soft Shore Protection. Coastal Systems and Continental Margins, vol 7. Springer, Dordrecht.

[3] Zhen-qing M. and Yong-he X. 2007. Effects of Water-Depth on Hydrodynamic Force of Artificial Reef. Journal of Hydrodynamics Ser.B. 19(3): 372-377.

[4] Zhaoyang J., Zhenlin L., Yanli T., Liuyi H., Dingyong Y. and Mansong J. 2010. Numerical Simulation and Experimental Study of the Hydrodynamics of a Modeled Reef Located within a Current. Chinese Journal of Oceanology and Limnology. 28(2): 267-273.

[5] Zhaoyang J., Zhenlin L., Yang L., Yanli T. and Liuyi. H. 2013. Particle Image Velocimetry and Numerical Simulations of the Hydrodynamic Characteristics of an Artificial Reef. Chinese Journal of Oceanology and Limnology. 31(5): 949-956.

[6] Woo J., Kim D., Yoon H.M. and Na, W.B. 2014. Characterizing Korean General Artificial Reefs by Drag Coefficients. Ocean Engineering. 82: 105-114.

[7] Kim D., Woo J., Yoon H.S., Na W.B. 2014. Wake Lengths and Structural Responses of Korean General Artificial Reefs. Ocean Engineering. 92: 83-91.

[8] Liu Y., Guan C. T., Zhao Y.P., Cui Y. and Dong G.H. 2012. Numerical Simulation and PIV Study of Unsteady Flow Around Hollow Cube Artificial Reef with Free Water Surface. Engineering Applications of Computational Fluid Mechanics. 6(4): 527-540.

[9] Liu Y., Zhao Y.P., Dong G.H., Guan C.T., Cui Y. and Xu T.J. 2013. Study of the Flow Field Characteristics Around Star-shaped Artificial Reefs. Journal of Fluids and Structures. 39: 27-40.

[10] Yaakob O.B., Ahmed Y.M., Jalal M.R., Faizul A.A., Koh K.K. and Zaid T.J. 2016. Hydrodynamic Design of New Type of Artificial Reefs. Applied Mechanics and Materials. 819: 406-419.

[11] Jiang Z., Liang Z., Zhu L., Liu Y. 2016. Numerical Simulation of Effect of Guide Plate on Flow Field of Artificial Reef. Ocean Engineering116: 236–241.

[12] Jiao L., Yan-xuana Z., Pi-hai G. and Chang-tao G. 2017. Numerical Simulation and PIV Experimental

Study of the Effect of Flow Fields around Tube Artificial Reefs. Ocean Engineering. 134: 96-104.

[13] Wang G., Wan R., Wang X., Zhao F., Lan X., Cheng H., Tang W. and Guan Q. 2018. Study on the Influence of Cut-Opening Ratio, Cut-Opening Shape, and Cut-Opening Number on the Flow Field of a Cubic Artificial Reef. Ocean Engineering. 162: 341-352.

[14] Lan C. and Hsui C. 2006. The Deployment of Artificial Reef Ecosystem: Modelling, Simulation and Application. Simulation Modelling Practice and Theory. 14(5): 663-675.

[15] Suzuki G., Kai S., Yamashita H., Suzuki K., Lehisa Y. and Hayashibar T. 2011. Narrower Grid Structure of Artificial Reef Enhances Initial Survival of In Situ Settled Coral. Marine Pollution Bulletin. 62(12): 2803-2812.

[16] Liu T.L. and Su D.T. 2013. Numerical Analysis of the Influence of Reef Arrangements on Artificial Reef Flow Fields. Ocean Engineering. 74: 81-89.

[17] Zheng Y., Liang Z., Guan C., Song X., Li J., Cui Y., Li., Q. and Zhou Y. 2015. Numerical Simulation and Experimental Study of the Effects of Disposal Space on the Flow Field around the Combined Three-tube Reefs. China Ocean Engineering. 29(3): 445-458.

[18] ANSYS Inc. 2016 ANSYS Fluent User's Guide, Release 17.2.